Golden Gate Bridge Response: A Study with Low-Amplitude Data from Three Earthquakes

Mehmet Çelebi,[a)] M.EERI

The dynamic response of the Golden Gate Bridge, located north of San Francisco, CA, has been studied previously using ambient vibration data and finite element models. Since permanent seismic instrumentation was installed in 1993, only small earthquakes that originated at distances varying between ~11 to 122 km have been recorded. Nonetheless, these records prompted this study of the response of the bridge to low amplitude shaking caused by three earthquakes. Compared to previous ambient vibration studies, the earthquake response data reveal a slightly higher fundamental frequency (shorter-period) for vertical vibration of the bridge deck center span (~7.7–8.3 s versus 8.2–10.6 s), and a much higher fundamental frequency (shorter period) for the transverse direction of the deck (~11.24–16.3 s versus ~18.2 s). In this study, it is also shown that these two periods are dominant apparent periods representing interaction between tower, cable, and deck. [DOI: 10.1193/1.4000018]

INTRODUCTION

THE BRIDGE

The Golden Gate Bridge (GGB) is an important lifeline connecting the City of San Francisco and the Peninsula in the south to Marin County in the north, serving more than 40 million vehicles per year. Completed in 1937, with a suspension span of 1,280 m (4,200 ft), the GGB reigned as the longest suspension span bridge in the world until 1964. With the approaches at both ends, the total length of the bridge is 2,737 m (8,981 ft). The two towers of the bridge are 210 m (689 ft) tall with respect to the top of the piers and are built of several cells composed of plates and angles that are braced by horizontal crossbeams. The width of the deck is 27.4 m (90 ft). A general schematic showing the dimensions of the suspension part of the bridge (excluding the approaches) is shown in Figure 1.

After the failure of Tacoma Narrows Bridge (WA) in 1940 due to severe torsional behavior of its deck during extreme wind conditions, concerns about the possible vulnerability of the GGB due to similar severe torsional behavior led to decisions in 1951 to implement the first important structural modifications to the bridge when some of the trusses that support the six-lane roadway were stiffened by adding wind braces (Abdel-Ghaffar and Scanlan 1985a, b, http://www.goldengatebridge.org/projects/retrofit.php [last accessed 10/18/2010], Vincent 1958, 1962a, b). Following the $M_w = 6.9$ 1989 Loma Prieta (CA) earthquake, additional

[a)] U.S. Geological Survey, Menlo Park, CA 94025

Earthquake Spectra, Volume 28, No. 2, pages 487–510, May 2012; © 2012, Earthquake Engineering Research Institute

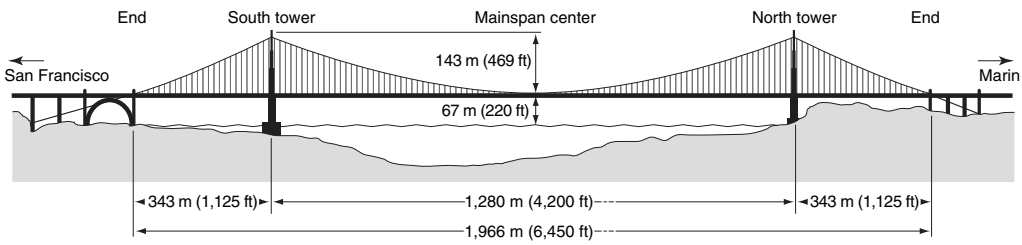

Figure 1. General schematic of the bridge depicting relative dimensions. (Figure updated and adopted from Ghaffar et al. 1985.)

vulnerability studies were carried out that identified that the bridge would not be safe in a future large earthquake (e.g., severe damages would be inflicted to the bridge during a M7.0 or greater earthquake occurring near the bridge, possible collapses of the approaches and severe damage to the suspension span occurring if the earthquake was M8.0 and larger. In 1992, an extensive seismic retrofit design was started according to site specific design ground motions associated with different magnitude earthquakes and performance levels (e.g., moderate earthquake defined as having 10% chance of exceeding in 50 years and having a peak acceleration of 0.46 g, and maximum credible earthquake defined as having 1,000-year return period or having peak acceleration of 0.65 g deemed to be similar to the 1906 San Francisco earthquake of M7.8) [http://www.goldengatebridge.org/projects/retrofit.php[1]]. Beginning in 1997, an extensive seismic retrofit of the bridge and its approaches started in phases. At the time of writing this paper, the retrofit of the approaches to the bridge has been completed, but the retrofit of the suspension bridge is planned to start in 2011. Hence, the data from the suspension bridge used in this paper reflect only the current response characteristics without the retrofit yet to be implemented. Data from either future earthquakes or tests will be needed to determine if the dynamic characteristics are significantly altered by retrofit on the suspension bridge. Hence, this and previous studies may serve as a baseline for comparison of the changes in dynamic response characteristics following the retrofit.

THE PAST INSTRUMENTS, TESTS AND ANALYSES

The dynamic response characteristics of the bridge have been identified and studied by others using both ambient vibration data and finite-element models. However, to the best knowledge of the author, this is the first study of the responses of the bridge to actual earthquake excitation input.

During and following construction, a limited number (maximum 10) of historical, bulky, heavy, and specifically designed accelerometers were deployed on the bridge, and various analyses have been performed using the non-earthquake (mainly vibrations due to wind) data obtained from those instruments (Vincent 1958, 1962a, b). Mathematical models of the

[1] Magnitude 7.8 is adopted from http://earthquake.usgs.gov/earthquakes/states/events/1906_04_18.php. The Golden Gate Bridge web-sites cites the magnitude as 8.3 which has been lowered by USGS to 7.8.

bridge have also been developed to estimate its various dynamic modal characteristics. Summarizing from Abdel-Ghaffar and Scanlan (1985a, b) and Vincent (1958, 1962a, b), the accelerometers were deployed by the U.S. National Geodetic Survey during and after construction of the bridge and later by the California Bureau of Public Roads. These early instrumental recordings continued intermittently until about 1954. Vincent (1958, 1962a, b) analyzed the instrumental data and compared them to mathematical models he developed. He found the vertical deck frequency to be about "8 cycles per minute" translating to a 7.5–second period and a torsional frequency of the deck about "12 cycles per minute" translating to a 5-second period. Later, Baron et al. (1976) made 3-D finite element analyses of the bridge. However, by far the most exhaustive ambient tests and analyses of data from such tests, as well as two- (2-D) and three-dimensional (3-D) mathematical modeling, have been carried out by Abdel-Ghaffar and Scanlan (1985a, b) and Abdel-Ghaffar et al. (1985). It is important to note that in the latter study, only 14 force-balanced accelerometers were used, and they were repeatedly deployed in arrays of limited spatial extent such that only a small subsection (e.g., one tower, or half of the main span and a side span) of the bridge was monitored at any given time. Given the limited number of sensors, this strategy helped them to better identify the mode shapes and numerous modal frequencies of these subsections.

Since these benchmark studies of 1985, in the 2005–2006 timeframe, studies on the bridge using ambient excitations with temporary deployment of sensors have been performed by Kim et al. (2007), Pakzad et al. (2008), Pakzad and Fenves (2009), and Pakzad (2010). These more recent studies had multiple purposes, including but not limited to design, developments, and the testing of a microelectricmechanical system (MEMS)-based wireless accelerometer nodes to develop as future structural health monitoring sensors, possibly for a variety of structures. To test these nodes, they have deployed a total of 64 nodes with two channels of accelerometers each, 56 on the main span and 8 on the south tower of the GGB. Each channel has been implanted with two different MEMS sensors, one to have better resolution at low-level motions and the other with high level motions. Numerous sets of ambient data with maximum amplitudes of about $\pm$ 10 mg recorded from the deck and south tower of the bridge have been transmitted through communications modules of the nodes at 50–200 samples per second for analyses using various methods including spectral analyses techniques and system identification methods. Pertinent results of their studies are included in the summary tables at the end of this paper to facilitate comparisons with results from those of Abdel-Ghaffar et al. (1985) and those obtained with earthquake data utilized in this paper.

The basic definitions of vibrational motions in a suspension bridge and primary mode shapes have been defined by Ghaffar et al. (1985), as shown in Figures 2 and 3. These descriptions are also used in this study.

OBJECTIVES AND SCOPE

In a previous paper (Çelebi 2010) preliminary results for the dynamic characteristics of the GGB were determined using data from three earthquakes, albeit with small amplitude motions, and compared to values from past ambient tests and theoretical analyses. In that paper, as well as this one, only selected results from earlier studies which are deemed to be pertinent are referred to when being compared to the more detailed analyses performed here. No mathematical models are developed in the current study. Spectral (Bendat and Piersol,

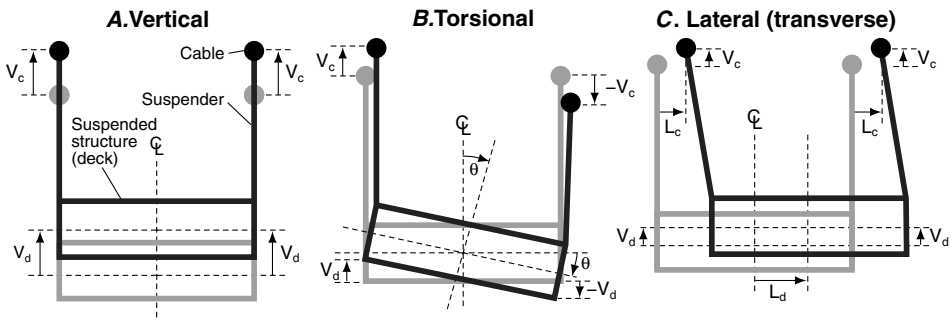

Figure 2. Basic vibrational motions of the deck of a suspension bridge, suspenders, and cable (modified from illustrations in Ghaffar et al. 1985).

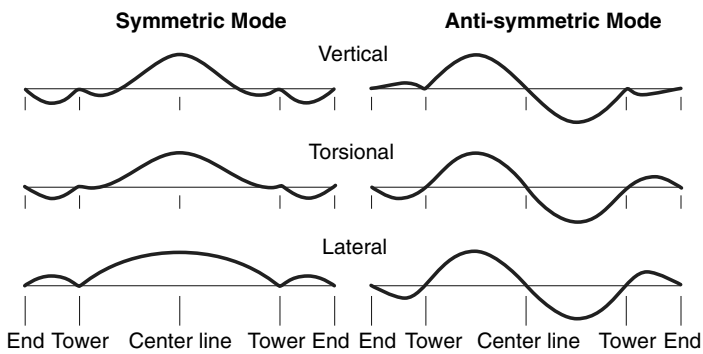

Figure 3. Basic symmetrical and antisymmetrical modes of a suspension bridge (condensed and reorganized from illustrations in Ghaffar et al. 1985).

1980) and system identification analyses (Ljung 1987, The MathWorks, Inc. 1988) are performed to identify relevant frequencies at different locations and along different orientations of the bridge in order to compare them to those reported in previous studies. Critical damping percentages determined by system identification analyses are very low and most likely are not reliable due to the low-amplitude motions, but nonetheless are reported later in this paper.

RECENT MODERN PERMANENT INSTRUMENTATION AND DATA

EARTHQUAKE DATA

In this paper, dynamic response characteristics of the GGB are identified using some of the limited number of earthquake response data acquired since the bridge was extensively instrumented after the 1989 Loma Prieta ($M_w = 6.9$) by way of an agreement between the Golden Gate Bridge Authority and the California Strong Motion Instrumentation Program (CSMIP) of the California Geological Survey (CGS). A general schematic depicting the deployments of sensors at the suspension part of Golden Gate Bridge is shown in Figure 4 (adopted from www.strongmotioncenter.org, last accessed 18 October 2010).

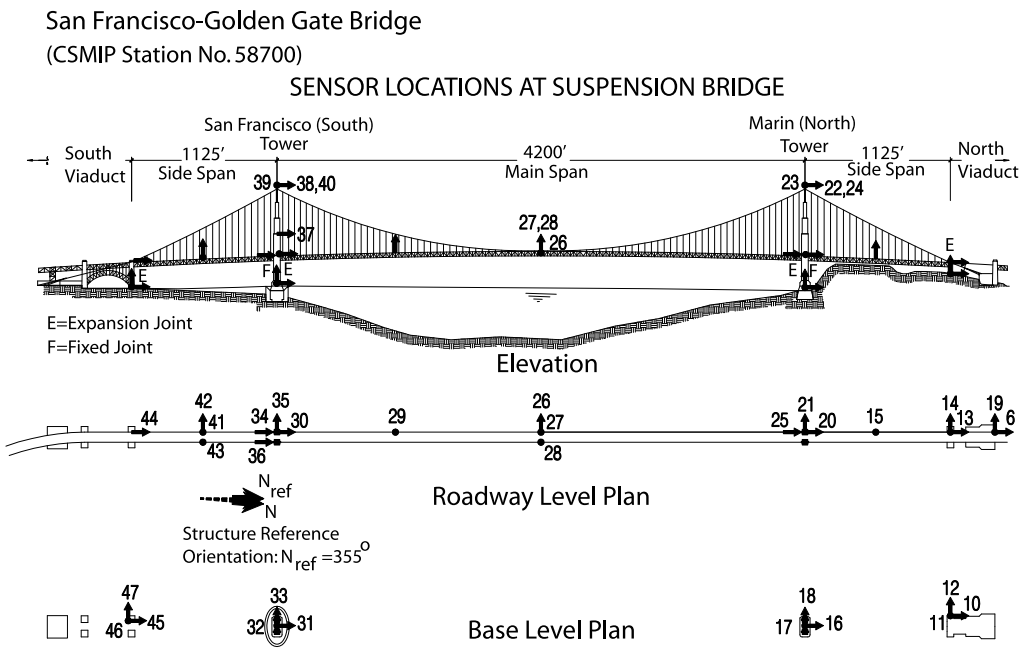

Figure 4. General schematic of the Golden Gate Bridge and associated instrumentation depicting sensor locations and orientations (adopted from http://www.strongmotioncenter.org, last accessed on 18 October 2010). Filled dots indicate channel orientation perpendicular to the paper (e.g., at roadway level), dots associated with the number 29 indicates channel 29 is vertical upwards at that location of the deck (as indicated in the plan view). Similarly, for Channels 27, 28, and 15.

The recently launched Center for Engineering Strong-Motion Data (CESMD) currently offers GGB response data from five different earthquakes (Figure 5). The figure also shows that among these events, the largest ground acceleration (2% g) and largest structural acceleration (11.2% g) were recorded during the Bolinas 1999 earthquake. Locations of the epicenters relative to the bridge are shown in Figure 6; note that the longitudinal direction of the bridge itself has a 355° azimuth with regard to true North. Azimuths from the epicenters of the earthquakes with regard to the center of the bridge, as well as other particulars of the recorded earthquakes, are summarized in Table 1.

In this paper, only three of the five earthquakes listed in Figures 5 and 6 are studied: Bolinas ($M_w = 4.5$), Yountville ($M_L = 5.2$), and Alum Rock ($M_w = 5.4$). The following are reasons for excluding some events:

1. Not all channels installed on the bridge (Figure 4) were recorded during each of these five earthquakes. Most of the important channels at significant locations of the bridge were recorded during the three selected earthquakes; hence, comparison and a check for consistency of the responses are possible.
2. The Gilroy data set has important channels missing (CH 15, 42, 26, 27, 28), and some of the important recorded channels (CH 38 and 39) did not record the earthquake signal properly. Hence, this earthquake data set is excluded.

CESMD Combined Strong-Motion Data

Home | Archive | Search | Help and Comment

Search

4 records match the followng search parameters

Station (City, Name or No): 58700 **Station type:** Bridge
PGA (g): Any **Epicentral Dist. (km):** Any

StaNo	Station	Network	Epic.(Fault) Dist. (km)	Horiz Apk (g)		Earthquake	View	Download
				Ground	Struct.			
58700	San Francisco - Golden Gate Bridge	CGS	20.9(--)	0.020	0.112	Bolinas99	○	□
	"		75.3(--)	0.012	0.036	AlumRock 30Oct2007	○	□
	"		122.3(--)	0.010	0.071	Gilroy 13May2002	○	□
	"		62.3(--)	0.009	0.039	Yountville 03Sep2000	○	□

Figure 5. List of available GGB earthquake response data from CESMD. (http://www.strongmotioncenter.org, last accessed 18 October 2010). However, as explained in the paper, Gilroy 2002 and San Francisco 2010 data sets are excluded in this study.

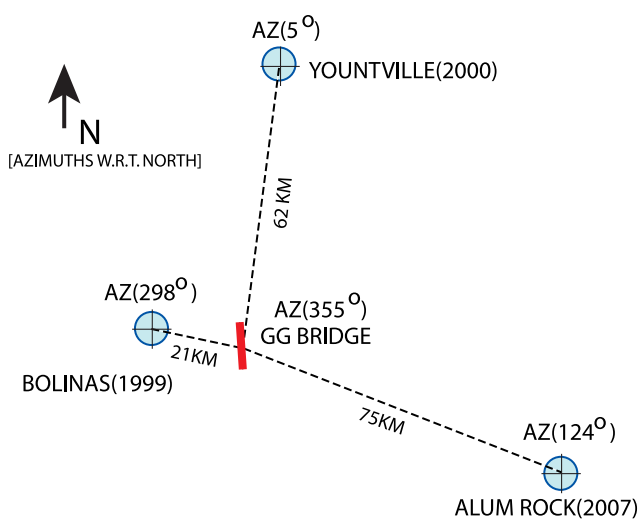

Figure 6. (a) General map showing locations of the Golden Gate Bridge (GGB) and the epicenters of the earthquakes recorded on the GGB array. (b) Azimuths from the mid-span of the bridge to the relative epicentral locations of the three earthquakes studied in this paper.

Table 1. Earthquakes recorded at the Golden Gate Bridge Array, San Francisco, CA (approximate distance and azimuth are obtained from the mid-span of the bridge to the epicenter of each event using Google Earth©; earthquake locations and magnitudes from USGS)

Golden Gate Bridge (37.818N, 122.477W)						
Earthquake	Date/Time UTC	Magnitude (M_w)	Depth (km)	Epicentral Dist.(km)	Coordinates (deg)	Azimuths (degrees)
Bolinas	8-17-1999/1:06	4.5	7.0	21	37.907N,127.686W	298
Yountville	9-3-2000/8:36	5.0	9.4	62	38.377N,122.414W	5
Gilroy	5-13-2002/05:00	4.9	7.6	122	36.967N,121.600W	141
Alum Rock	10-30-2007/03:04	5.4	9.2	75	37.432N,121.776W	124
Offshore San Francisco	6-28-2010/14:47	3.3	8.0	11	37.74N,122.56W	212

3. The most recent San Francisco (2010) earthquake is excluded because the motions are too small and impulsive to trigger significant responses in the lower frequency modes of the bridge.

Because the processed data served from the CESMD exhibits considerable variation in processing parameters, in this paper, the unfiltered versions of the acceleration time series data (available at 200 sps) for the selected earthquakes are re-processed (with 200 sps) using a much wider filtering bandwidth (0.05–50 Hz, a causal Butterworth filter with a roll off factor of 2) in order not to exclude longer-period modes of the bridge suggested by previous studies.

ANALYSES OF EARTHQUAKE DATA

Summary Plots of Accelerations, Displacements and Amplitude Spectra

Thirty-nine channels of accelerometers deployed at the base level, roadway (deck) level and towers of the suspension part of the GGB are depicted in Figure 4. In order to study the data from the three earthquakes, first, summary plots of time-histories and amplitude spectra (Figures 7–10) are developed to visualize relative amplitudes and to understand general behavior and dynamic characteristics.

Figure 7 shows plots of time-histories of band-pass filtered accelerations recorded at GGB from the three earthquakes: Bolinas 1999, Yountville 2000 and Alum Rock 2007, arranged as a column of three frames for each earthquake, respectively. In each frame of a column for one of the earthquakes, acceleration time-series are plotted for pertinent channels at different locations of the bridge in the transverse, longitudinal, and vertical directions of the bridge, respectively. Out of 39 accelerometers of the suspension part of the bridge (Figure 4), time-series for 32 pertinent channels, if recorded for each earthquake, are plotted. It is noted herein that the lengths of the records for all of the earthquakes studied herein are not equal. Furthermore, to better visualize, the first 20 seconds of the Alum Rock record is not included in this plot for that earthquake.

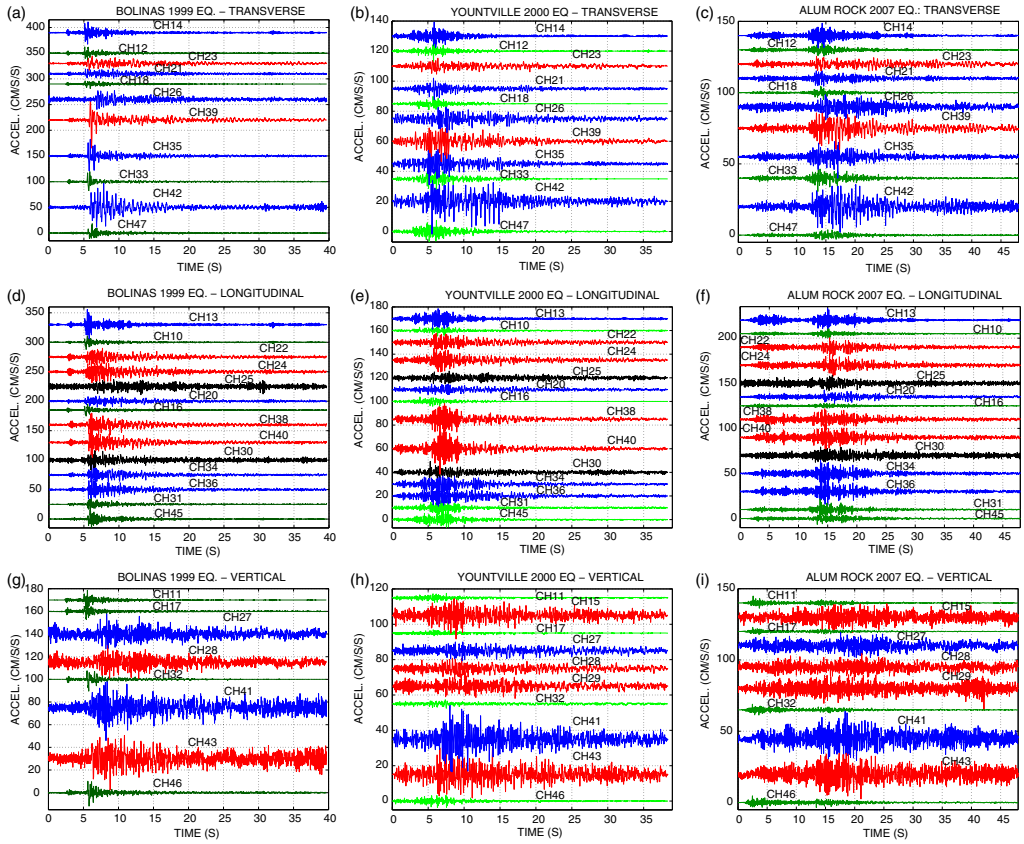

Figure 7. Time-histories of band-pass filtered accelerations recorded at key locations on the Golden Gate Bridge for three earthquakes. (a) Bolinas 1999; (b) Yountville 2000; (c) Alum Rock 2007. In each column, the top row shows the transverse, the middle row shows the longitudinal, and the bottom row shows the vertical direction of motion of the bridge. (Note 1: Record lengths of the earthquakes are not equal; e.g., for plotting purposes, the first 20 seconds of the Alum Rock record is not included in this plot. Note 2: For the Bolinas earthquake, CH15 is missing from the data set. Note 3: For easier comparison, all time-series in each plot are equiscaled but zero axis of each channel y-axis is shifted for easier visual comparison). Colors in the figures do not follow any particular scheme.

Clear interpretations and/or conclusions cannot be derived from the acceleration plots alone except to note the relative amplitudes of accelerations at key locations in the transverse, longitudinal and vertical directions of the bridge. It is noted that, consistently:

1. In the transverse direction, the largest accelerations of the bridge occur at the center of the south side-span (CH42), rather than on the deck main span center (CH26). Because there is no accelerometer in the transverse direction at the center of north side-span, the motions at this location are unknown, which precludes direct identification of the symmetrical or unsymmetrical modes of the side span as shown in

Figure 3. However, as shown later in the summary displacement time-histories, this does not necessarily translate into largest displacements (or relative displacements) at the center of the side-span. Also, the accelerations at the top of the north tower (CH23) are smaller than that at top of south tower (CH39).

2. In the longitudinal direction, the accelerations at the north tower top (CH22 & CH24) are smaller than those at the south tower top (CH38 and CH40). This is more so for the Yountville and Alum Rock earthquakes as compared to the Bolinas earthquake.
3. In the vertical direction, the accelerations at the center of the south side-span (CH41 and CH43) are larger than those at the center of main-span (CH27 and CH28), as is the case for transverse motions, as well as those at the center of north side-span (CH15). (Note that CH15 was not recorded during the Bolinas earthquake.) Again, the way these observations compare for displacements at these locations is discussed later in the paper.

In Figure 8, amplitude spectra computed from accelerations are shown for the three earthquakes. From these plots the following observations are made:

1. Even though some peaks in the vicinity of 1 Hz are visible, in general, some of the lower-frequency (longer-period) modes of the bridge (e.g., transverse direction in particular) are difficult to identify from amplitude spectra computed from accelerations as in Figure 8. This is not very unusual situation as signal to noise ratio is smaller for small amplitude shaking than for strong shaking and amplitude spectra of accelerations usually does not point out the lower frequency peaks as well.
2. On the other hand, the vertical frequency of the center deck and the longitudinal frequencies of the two tower tops, all at about ~0.12–0.13 Hz are clearly identifiable for both the Bolinas and Alum Rock data sets.
3. The vertical and transverse frequencies of the deck are dominant frequencies that appear in other spectra (e.g., longitudinal and transverse tower response) and, as discussed later, are inferred to be due mainly to interaction between the deck, cable, and tower. Furthermore, as shown later, application of the system identification method can only extract this frequency.
4. Amplitude spectra of vertical accelerations at the center of the deck main-span (CH27 and 28) are repeated also in the frames displaying spectra of longitudinal channels of tower (CH22, 24, 38, and 40) to show that they all share the ~0.12 Hz lowest frequency due to interaction between the deck and towers via the cables and suspenders.

Similar to Figure 7, Figure 9 shows displacement time-histories computed by double-integration of the band-pass filtered accelerations

Similar to Figure 8, Figure 10 shows amplitude spectra computed from displacements[2] recorded at key locations in the transverse, longitudinal, and vertical directions of the bridge for the three earthquakes. As mentioned before, amplitude spectra computed from displacements preferentially emphasize lower frequencies. In order to achieve higher and

[2] This figure is plotted with horizontal axis 0-1 Hz in order to better display the lower frequencies. No significant peaks are displayed (not presented) when plotted for 1–2 Hz.

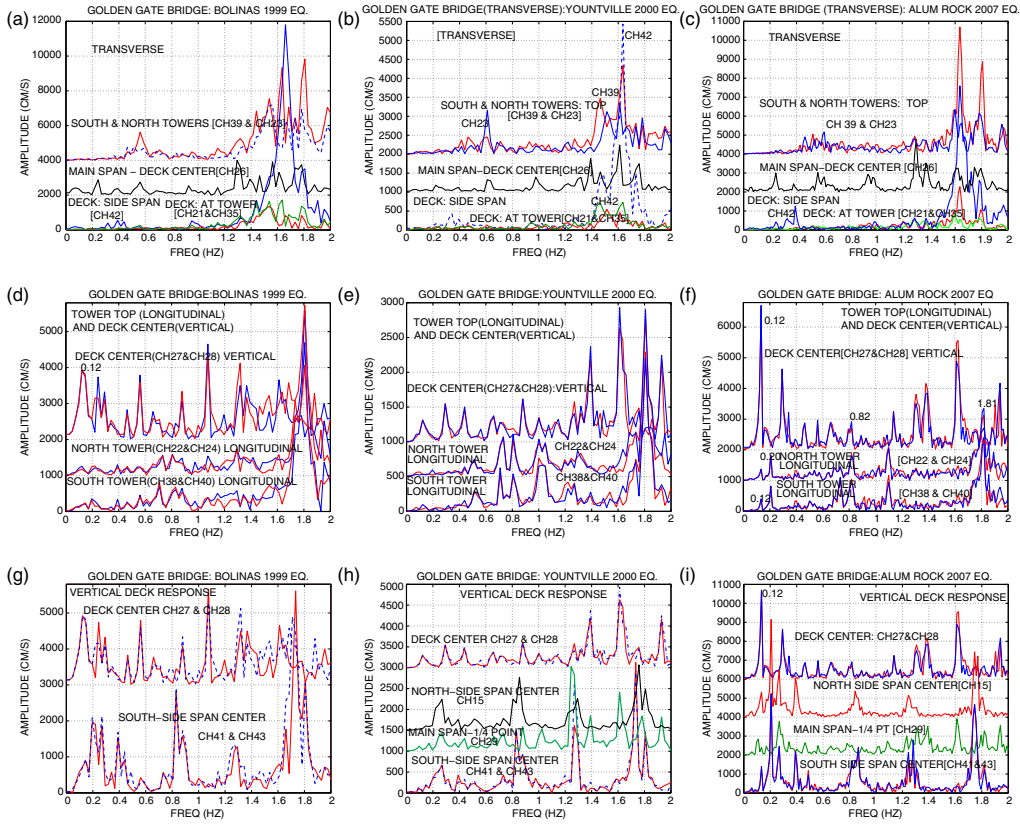

Figure 8. Amplitude spectra computed from accelerations recorded at key locations of Golden Gate Bridge for three earthquakes (a) Bolinas 1999; (b) Yountville 2000; (c) Alum Rock 2007. For each column (earthquake) the top row shows transverse, the middle row shows longitudinal, and the bottom row shows vertical directions of the bridge. (Note that for each earthquake, the actual record length, padded with zeros to 24,000 data samples, is used for computing amplitude spectra. Also, for the Bolinas earthquake, data from Channels 15, 19, and 29 are missing, and for the Yountville earthquake, data from Channels 19 and 44 are missing).

consistent resolution at low frequencies, the amplitude spectra were computed using the actual record length for each earthquake (varying between 7,000–13,000 points) padded with zeros at the tail end up to 24,000 points, or a duration of 120 s. Thus, the effective resolution is 0.0083 Hz.

As was done for accelerations, amplitude spectra of vertical displacements at center of deck main-span (CH27 and 28) are repeated also in the frames displaying spectra of longitudinal channels of tower (CH22, 24, 38, and 40) to show that they all share the 0.12 Hz lowest frequency due to interaction between the deck and towers via the cables and suspenders.

The group of frames for transverse direction in the top row of Figure 10 illustrate consistently for the three earthquakes the lower frequency 0.06–0.07 Hz (14.3–16.3 s) at the

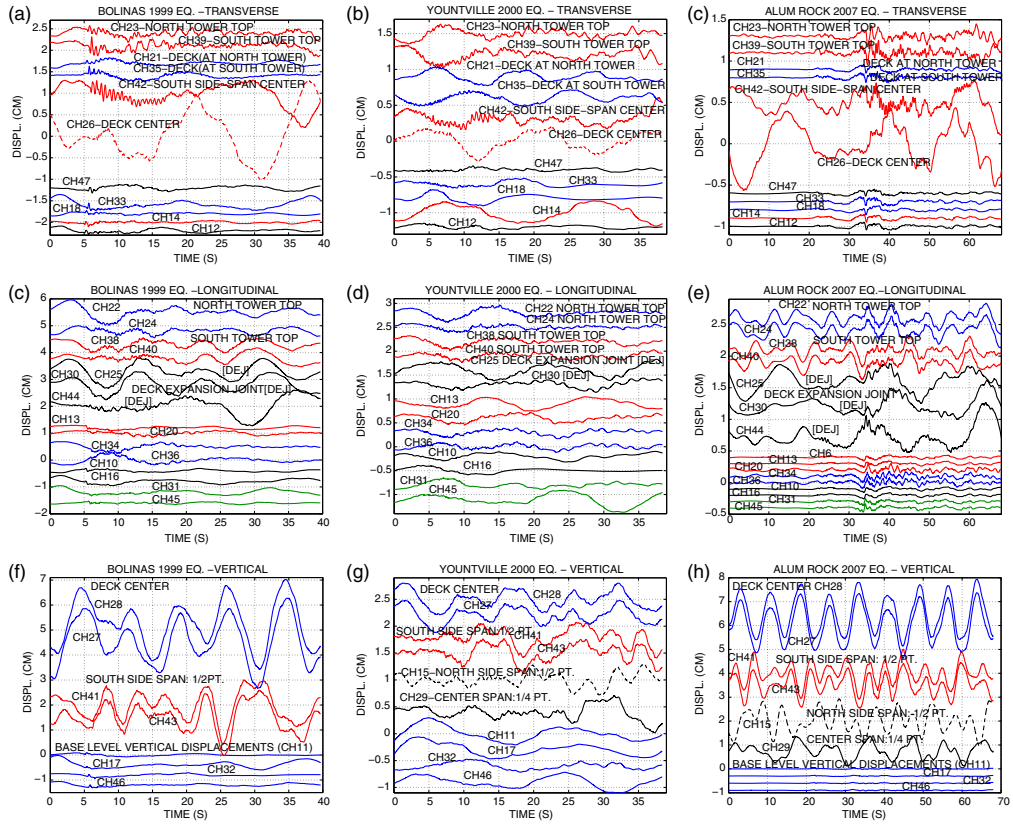

Figure 9. Time-histories of displacements computed by double-integration of band-pass filtered accelerations recorded at key locations of Golden Gate Bridge from the (a) Bolinas 1999, (b) Yountville 2000, and (c) Alum Rock 2007 earthquakes in the (1) top row: transverse, (2) middle row: longitudinal, and (3) right row: vertical direction of the bridge, respectively. (Note: (i) Record lengths of the earthquakes are not equal, (ii) to better compare displacements at key locations, the sequence of appearance of channels have been changed and are not in the same order as those in the accelerations plots, (iii) For Bolinas earthquake, data from Channels 15, 19, and 29 are missing. For the Yountville earthquake, data from 19 and 44 are missing).

tower tops (CH23 and CH39) which is the same as that of the center of deck in the vertical direction (CH26), as well as the deck at tower locations (CH21 and CH35) due to interaction. However, in the transverse direction, there are clear indications of 0.5–0.6 Hz (1.67–2.0 s) frequency only for the towers. As shown later, this frequency is that of the tower only. The frequency at 0.06–0.07 Hz is the apparent transverse frequency of the deck and towers interacting and is the same as that of the deck as explained later in the manuscript. This was discussed by Abdel-Ghaffar and Scanlan (1985a, b) only briefly and only as a possibility.

In the middle row of the group of frames in Figure 10, for all the three earthquakes, although the intent is to identify longitudinal frequencies of the tower, the vertical spectra

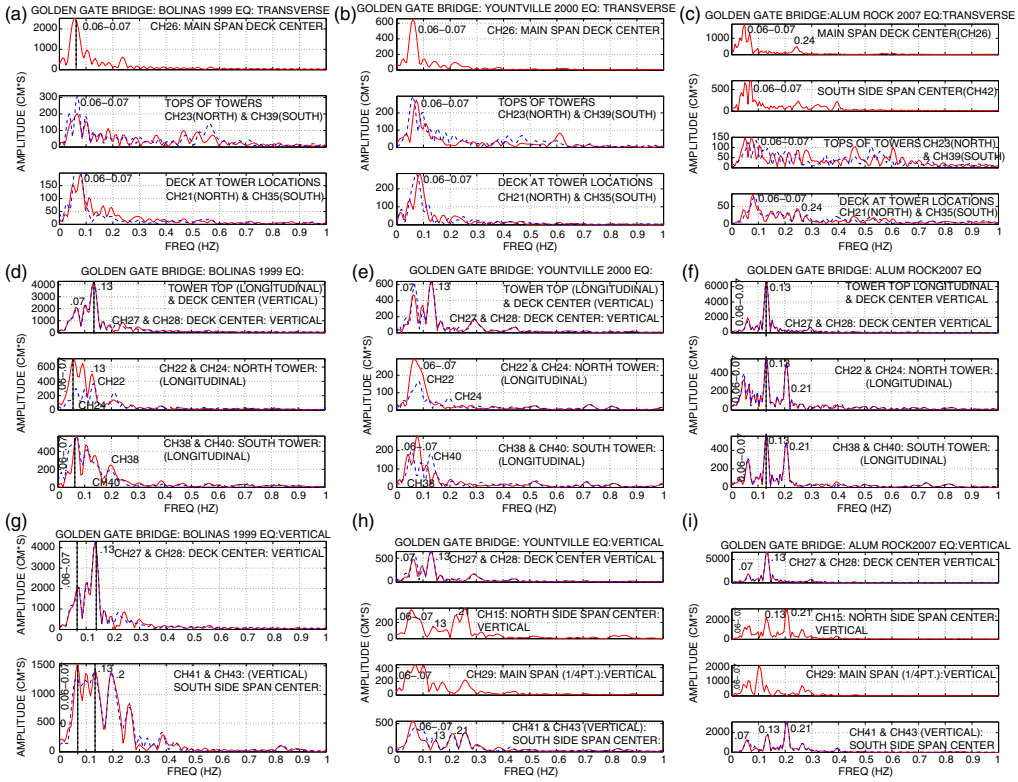

Figure 10. Amplitude spectra computed from displacements at key locations on the Golden Gate Bridge. (a) Bolinas 1999, (b) Yountville 2000, (c) Alum Rock 2007, earthquakes. *Top row:* transverse, *Middle row:* longitudinal, *Bottom row:* vertical directions of the bridge. See text for detailed discussion of how amplitude spectra are computed. Note that for the Bolinas earthquake, data from Channels 15, 19, and 29 are missing, and for the Yountville earthquake, data from Channels 19 and 44 are missing.

of the center of deck main span is also included to show the effect of interaction. The 0.13 Hz frequency (7.7 s period) that appears in all deck center vertical spectra also appears in the spectra of longitudinal motions of the tower tops, indicating that the apparent frequency of interaction is the same as that of the deck. This is normal because the towers in the longitudinal direction are very stiff compared to the vertical stiffness of the deck main span.

In addition, Figure 10 shows, for example, two spectra computed from displacements for the Yountville (2000) earthquake, which clearly illustrate the fundamental frequency (period) of interaction—lowest at 0.06-0.07 Hz (period 14.3–16.3 s)—for the towers in the longitudinal direction and for the deck center in the vertical. Possible second deck center (CH27 and 28) vertical mode frequency (period) at 0.22–0.24 Hz (4.17–4.55 s) is also clearly identifiable from the spectra in Figure 10 (center column, top row group of frames) but also as the vertical frequency corresponding to the north side span (CH15-vertical), south side span (CH14 and 43-vertical), main deck quarter point (CH29). A second dominant frequency at

0.22 Hz (period 4.55 s) is also common to both towers and the deck center and is the frequency at second mode of the deck in the transverse direction or appears there because of interaction or torsion. Results for the Alum Rock (2007) and Bolinas (1999) earthquakes are similar.

Both the displacement time-histories in Figure 9 and subsequent spectral analyses reveal the following:

1. In the transverse direction, during all three earthquakes, the largest displacements occur at the main deck center (CH26). This observation is not surprising when, for the first mode, the longer length of the main span as compared to those of the side spans is considered.
2. The phases of displacements at comparable locations of the bridge are not the same for all three earthquakes. For example:
   a. In the transverse direction for the Alum Rock earthquake, the responses at the two tower tops (CH23 and CH39), the deck at tower locations (CH21 and CH35), and all of the locations below the deck (Channels 47, 33, 18, 14, and 12) are in-phase for most of the shaking. Responses at locations below the deck also appear to be in-phase and are separately discussed later in this section. In contrast, for the Yountville earthquake, the responses at the tower tops and the deck at tower locations are (approximately) 180º out-of-phase for most of the shaking. This is also confirmed by the coherence and phase angle, as well as cross-spectrum at the two (north [CH23] and south [CH39]) tower top locations (Figure 11). Although coherencies are not high, it is clearly seen that while the two towers are in-phase at 0.5–0.6 Hz during the Alum Rock and Bolinas earthquakes. They are about 180º out-of-phase during the Yountville earthquake. This confirms the displacement time-history plots that exhibit for the Yountville earthquake the out-of-phase displacements of the two towers. The lower frequency peak at about 0.06–0.07 Hz is the tower-cable-deck interaction frequency discussed previously and displayed in the summary amplitude spectra plots in Figure 10 and later in the paper.

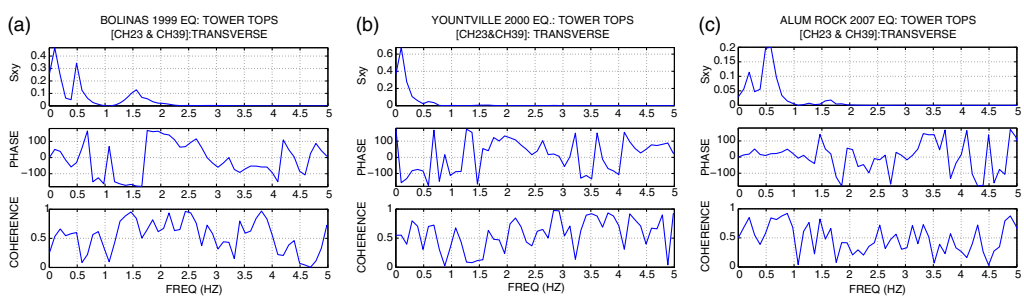

Figure 11. Cross-spectrum, phase angle and coherency plots for the transverse direction of the South (CH23) and North (CH39) tower tops for (a) Bolinas, (b) Yountville and (c) Alum rock earthquakes. For the Bolinas and Alum Rock earthquakes, tower tops are in phase at 0.5-0.6 Hz, a frequency unique to the towers. For the Yountville earthquake, the tower tops are out of phase by 180º at that frequency,. The peak at lower frequencies between 0.05-0.12 is characteristic of the deck, and appears in these plots because of interaction between the deck and towers.

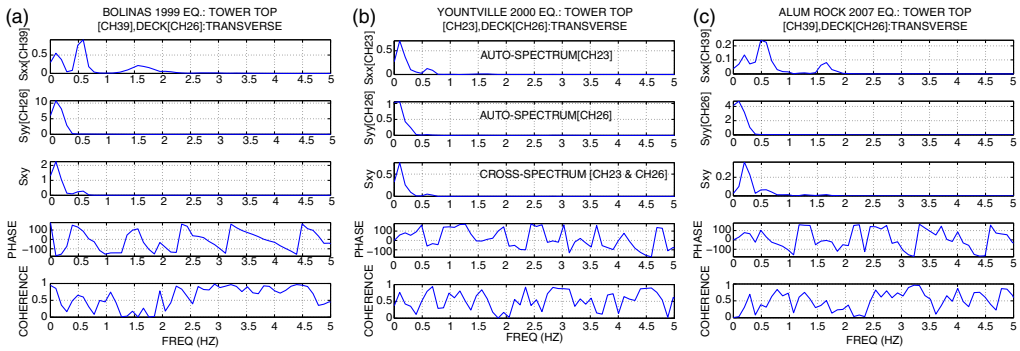

Figure 12. Auto and cross-spectra, phase-angle, and coherency plots for the transverse direction of the tower tops [CH39 for (a) Bolinas and (c) Alum Rock, and CH23 for (b) Yountville earthquakes] versus the center of deck main span (CH26). Auto-spectra at the tower tops clearly show a peak at 0.5–0.6 Hz that does not appear in auto-spectra of the deck center; hence this frequency belongs to the towers only. Coherencies are not high and phase changes for each earthquake. The lower frequency between 0.05–0.12 Hz belongs to the deck and appears in all spectra because of tower-cable-deck interaction.

In Figure 12, comprehensive auto and cross spectra, as well as phase and coherence plots for pairs motions at the tower tops (CH39 for Bolinas and Alum Rock, and CH23 for Yountville earthquakes) versus the center of deck main span (CH26), are presented and illustrate that auto-spectra at the tower tops clearly shows 0.5–0.6 Hz that does not appear in auto-spectra of the deck center; hence this frequency belongs to the towers only. Coherencies are not high and the phase relationship changes for each earthquake. The lower frequency between 0.05–0.12 Hz belongs to the deck and appears in all spectra because of tower-cable-deck interaction.

b. In the case of the Bolinas earthquake, the transverse direction phase situation for comparable locations are not visually clear in these summary displacement time-history plots.

c. It is therefore likely that such differences are due to directionality effect of the input motions to the structure as indicated by the azimuths from main-span deck center to the epicenters of the earthquakes (Table 1, Figure 6). For example, for the Alum Rock earthquake, motions from the epicenter (with azimuth, from the epicenter to the center of main-span of approximately 304º, or from the center of the main-span to the epicenter of 124º) first hit the south end of the bridge and, with a time-delay (although small), propagate toward the north, and this is observed in the displacement response time-histories (Figure 13). However, it is noted that there is a very small, if any, time-delay between the south end and north ends of the main suspension length, both at base level and roadway level and between the two levels. This may well explain why the tower tops are in phase during most of the shaking and is attributable to the azimuth of the epicenter with respect to the bridge and as a result the directionality of incoming motions—which, in this case, are mostly strong in radial direction. For the Yountville earthquake (with the azimuth from epicenter to the center of main-span of approximately 185º, or from the center of main-span to the

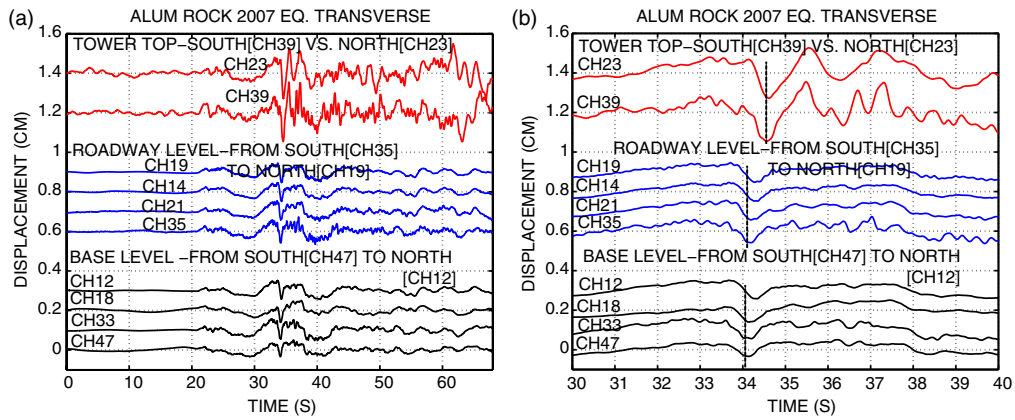

Figure 13. (a) Wave propagation of transverse motions are displayed from base level to tower top during the Alum Rock earthquake. Right: ten seconds (between 30–40 seconds into the record) shows delay time of about 0.4–0.5 seconds from base and roadway level to tower top. The tower top clearly exhibits mostly in-phase and approximately 2 s (0.5 Hz) displacements during the strongest part of shaking between 30–40 seconds into the record.

epicenter of 5º) surface waves reach most of the base level locations in the transverse direction of the bridge with phase differences (deducted from time-history plots of Channels 12, 14, 18, 33, and 47 (Figure 10, top row center frame) between south and north ends and hence the possible reason for the phase difference in the tower responses.

d. In the longitudinal direction displacement time-history plots (Figure 9), the reverse is observed; that is, the tower tops are in-phase for the Yountville earthquake but out-of-phase (approximately 180º for the Alum Rock earthquake. In more detail, Figure 14 illustrates again for the Alum Rock earthquake how the incoming waves propagate in the longitudinal direction from the base (channels 45, 31, 16, 100) to roadway level (channels 36, 34, 20, 13, 6) and then to the tower tops (channels 38 and 40 and 22 and 24). As seen, there is approximately 0.3–0.4 s time-delay between the south end and north ends of the main suspension length, both at base level and roadway level, as well as between the two levels. Hence, this may have caused the out-of-phase behavior at the tower tops in the longitudinal direction during this earthquake. This clearly is attributed to the directionality (azimuth of the epicenter with regard to the bridge). Again, no clear deduction can be made for the Bolinas earthquake.

3. Not too much can be interpreted from the limited data for the longitudinal deck response, since both ends of the deck main span have expansion joints. At the deck main span, and except for Channels 25 (north end) and 30 (south end), there are no accelerometers in the longitudinal direction of the deck. Nonetheless, Figure 15 shows, only for the Alum Rock 2007 earthquake, amplitude spectra of all channels in the longitudinal direction of the deck (roadway level) main span and side-spans. The significant frequencies in the spectra belong to the interacting tower-cable-deck system. However, the ~0.2 Hz frequency appears as also the

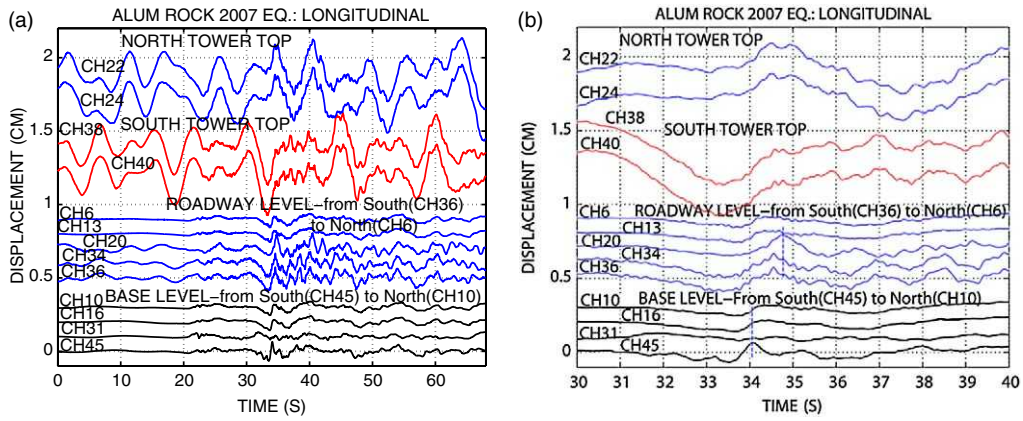

Figure 14. (a) Wave propagation of longitudinal motions are displayed from base level to roadway level during the Alum Rock earthquake. (b) Ten seconds (between 30–40 seconds into the record) shows delay time of about 0.3–0.4 seconds from south end toward north end. This delay may have caused the out-of-phase motions at tower tops in the longitudinal direction appearing to be around 7–8 s as seen in time-histories.

frequency of the deck of the two side-spans. With the available data, no specific frequency can be assigned to the deck main span; however, the deck main span clearly contains the aforementioned dominant interaction frequencies. This trend is similar for the other two earthquakes.

4. The displacements or the relative displacements in the transverse direction at deck center computed from accelerations for the 3 earthquakes are not similar as

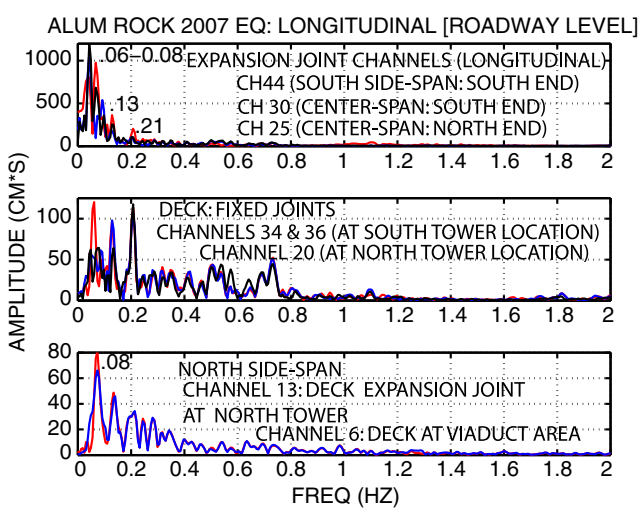

Figure 15. Amplitude spectra of the displacement response in the longitudinal direction of the roadway level for the Alum Rock earthquake. In general, coincident colors indicate coincident frequencies for the grouped channels in each frame.

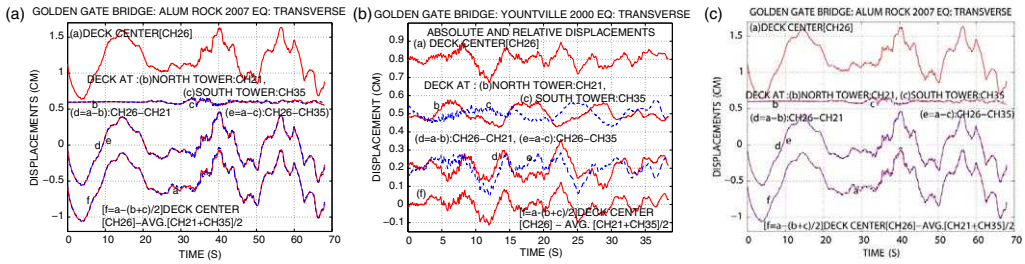

Figure 16. Equiscaled absolute and relative displacements at the deck center and deck at tower locations for the three earthquakes. When there are two colors, the first channel identified in the text of the figure is represented by "red" color.

displayed in Figure 16 that shows the displacement time-histories from the three earthquakes. In addition, for each earthquake the deck center absolute displacement is similar both in shape and phase to the relative displacement computed with respect to the deck locations at tower position. Hence, for small amplitude earthquake data, the absolute displacement at deck center can be considered the same as the relative displacement at deck center with respect to the deck at tower locations.

Note on Interaction Apparent Frequency

In this section, the terminology and relationship for "apparent" frequency, similar to those used in soil-structure analyses in buildings $[1/f^2_{apparent} = 1/f^2_1 + 1/f^2_2$ or $1/f^2_{apparent} = 1/f^2_1 + 1/f^2_2]$, is adopted (Jacobsen and Ayre 1958, Luco 1986, Trifunac et al. 2001). Trifunac et al. (2001) describe this relationship as a "combination rule" whereby apparent frequency, f_a, (period, T_a) is shorter (longer) than the shortest frequencies (longest periods) of interacting parts. However, in case of Golden Gate Bridge (as may possibly be for all long-span suspension bridges), when, for example only deck (f_{deck}) and tower (f_{tower}) are considered, the difference between them are so large that the apparent frequency is identical to the lower of the two–which always is the deck.

The apparent frequency (f_a) at 0.13 Hz for the interacting tower longitudinal (~0.7 Hz average by itself) and deck vertical (0.13 Hz) motions is the same as the deck vertical (0.13 Hz), also computed by $[1/f^2_a \sim 1/.7^2 + 1/.13^2]$. Similarly, the apparent tower transverse frequency f_a is 0.06–0.07 (by itself ~0.45 Hz) by the same relationship $[1/f^2_a \sim 1/.07^2 + 1/.45^2]$. This explains why these apparent frequencies are so dominant and appear not only in the deck but also in the tower responses.

Torsion

Torsion of the towers and deck center-span and deck side-span can, in principal, be determined using data recorded by pairs of two parallel accelerometers at appropriate locations of the bridge (e.g., in the longitudinal direction, CH 22 and 24, and CH38 and 40 at the tops of the north and south towers respectively; in the vertical direction of the deck, Channels 27 and 28 at the center of mid-span, and Channels 41 and 43 at the south side-span). The difference between each pair represents the relative torsional displacement.

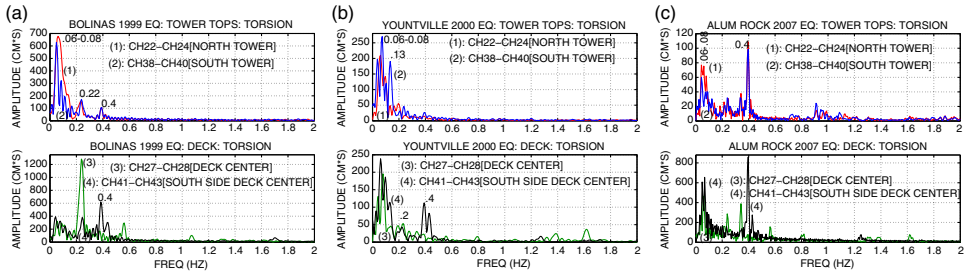

Figure 17. Amplitude spectra of relative torsional displacements computed from relative displacements between pairs of parallel displacements (a) in the longitudinal direction at the tops of the two towers and (b) in the vertical direction of the centers of deck main span and south side span. Colors do not specify any particular distinction.

Although it is not a main objective of this study, exact torsional rotation could be computed by dividing the relative torsional displacement by the exact distance between the locations of the pair of the parallel sensors. Figure 17 presents the relative torsional amplitude spectra computed using the relative displacements between each pair discussed. As seen in this figure, the spectra have several frequency peaks in common, although some are more pronounced than others. That the vertical deck frequency (~0.06–0.08 Hz) appears in all torsional computations is a strong indicator of mode coupling between the deck-vertical and tower-longitudinal motions, which likely occurs via cable interactions as described previously. The relative amplitude of the frequency peak at about ~0.4 Hz, however, is not very large at the center of the deck main-span, but is very large at the center of the south side span (particularly for the Alum Rock earthquake) as well as at the tops of the towers. Thus, these plots do not show any clear torsional frequency for the main-span deck. However, since ~0.4 Hz frequency is not predominant in the amplitude spectra of individual channels (Figure 10), it is possible that it belongs to the torsional mode of the deck south side-span.

The lack of a pair of accelerometers on the north side-span prevents the determination of whether this is a symmetric or an antisymmetric mode of the deck side-spans as described in Figure 3. Furthermore, the same 0.4 Hz frequency is predominant in the relative torsional amplitude spectra of the towers, particularly for the Bolinas and Alum Rock earthquakes. Sample auto-spectra and cross-spectrum of pairs of relative torsional motions from the Alum Rock earthquake (CH22–CH24 for the North Tower and CH3–CH40 for the South Tower) presented in Figure 18 validate clearly the in-phase and highly coherent ~0.4 Hz torsional frequency of the towers.

System Identification

To better identify mode shapes corresponding to the numerous frequencies determined by spectral analyses of the response data, system identification analysis was performed on selected data to identify key frequencies and possibly validate those determined by spectral analyses. A model is estimated using appropriate pairs of observed responses (accelerations or displacements) are used as single-input, single-output. The auto-regressive extra input (ARX) model based on least squares method is used in this analysis. The reader is referred to Ljung (1987) and *MATLAB User's Guide* (The MathWorks, Inc. 1988 and newer versions)

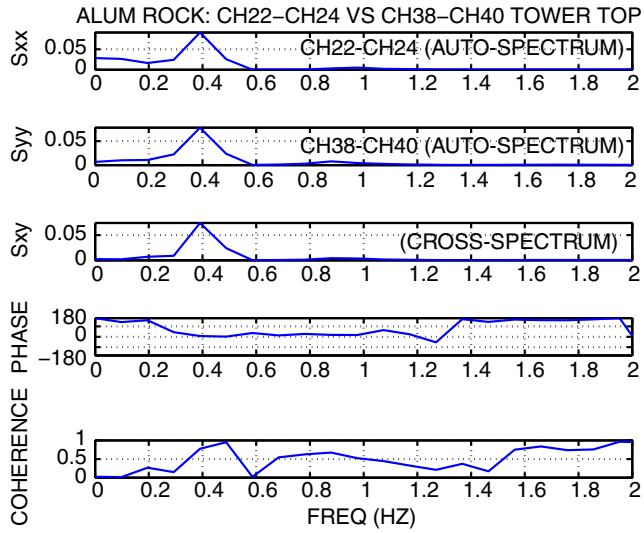

Figure 18. Sample auto- and cross-spectra, phase angle, and coherency plots for the relative torsional displacements at the tower tops (CH22–CH24 for North tower and CH38–CH40 for the south tower) for the Alum Rock earthquake. Note the clear peaks in the spectra and coherence at about ~0.4Hz, where the phase is 0; these are interpreted to be at the torsional frequency of the towers.

for detailed formulations of the ARX and other system identification models. Possibly due to the low signal-to-noise ratios that characterize these data, as compared to higher rations typical for stronger shaking, it was difficult to identify many of the higher modes. However, some of the key frequencies for four of the important modes were identified along with the corresponding modal damping ratios. These results are summarized in Table 2.

COMPARISON OF DYNAMIC CHARACTERISTICS

Table 3 summarizes the modal fundamental frequencies identified (some less well determined than others) in this study and compares them with selected results from two other prior

Table 2. Fundamental frequencies (f) [and corresponding periods (T)] and associated damping percentages (ξ) obtained by system identification analyses of the responses recorded for the three earthquakes in this study

Location	Bolinas 1999		Yountville 2000		Alum Rock 2007	
(Direction)	f(hz)[T(s)]	ξ (%)	f(hz)[T(s)]	ξ (%)	f(hz)[T(s)]	ξ (%)
Deck(Transverse)	.093 [11.75]	.34	.095 [10.52]	.48	.089 [11.24]	.85
Tower(Transverse)	.53 [1.89]	.1	.70 [1.43]	.27	.56 [1.78]	.08
Deck(Vertical)	.13 [7.69]	.2	.13 [7.69]	.27	.13 [7.69]	.07
Tower(Longitudinal)	.139 [7.19]	.18	.124 [8.06]	.41	.15 [6.66]	.11

Table 3. Comparative summary of fundamental frequencies in Hz (periods, in seconds) from past and current studies

	Abdel-Ghaffar et al. (1985)[1]		Kim et al. (2007), Pakzad et al. (2008, 2009), Pakzad (2010)		This Study: Earthquake Data (2010)		
					Spectral Analyses		
					System Identification		
Location (Direction)	Ambient	FE[2]	Ambient	FE	Bolinas 1999	Yountville 2000	Alum Rock 2007
Deck (Transverse)	0.055 (18.2)	.049–.064 (15.6–20.4)	0.228[5] (4.39)		0.06–0.07 (14.3–16.3)	0.06–0.07 (14.3–16.3)	0.06–0.07 (14.3–16.3)
					.093 (11.75)	.095 (10.52)	.089 (11.24)
Deck Center Span (Sym. Mode) (Vertical)	0.122 (8.2)	.124–.127 (7.9–8.1)	0.106[5] (9.41)	0.095 (10.55)	0.12–0.13 (7.7–8.3)	0.12–0.13 (7.7–8.3)	0.12–0.13 (7.7–8.3)
					0.13 (7.69)	0.13 (7.69)	0.13 (7.69)
Towers (alone)[3] (Transverse)	0.46 (2.18)	0.43 (2.30)	0.24 (4.17)		0.5–0.6[3] (1.67–2.0)	0.5–0.6[3] (1.67–2.0)	0.5–0.6[3] (1.67–2.0)
					0.53[3] (1.89)	0.70[3] (1.43)	0.56[3] (1.78)
Towers[4] (Longitudinal)	0.75 (1.33)	.66–.69 (1.44–1.52)	0.583 (1.72)		0.12–0.13 (7.7–8.3)	0.12–0.13 (7.7–8.3)	0.12–0.13 (7.7–8.3)
					0.139 (7.19)	0.124 (8.06)	0.15 (6.66)
Suspension Deck (Longitudinal)	0.262 (3.81)		N/A		Inconclusive		
Side-Spans (Deck) (Longitudinal)			N/A		~0.2-0.24		
Tower (Torsional)	0.82 (1.21)	0.91 (1.10)	0.93 (1.08)		0.4 (2.0)	0.4 (2.0)	0.4 (2.0)
Deck (Torsional)	0.24 (4.10)	.21–.22 (4.53-4.72)	0.229 (4.37)	0.186 (5.37)	Inconclusive		

(1) Limited summary of the modes by Abdel-Ghaffar et al. (1985) is also summarized in Chopra (1996).
(2) FE=Finite Element Modal analyses: variation due to 2 or 3 dimensional modeling.
(3) It was possible to identify the transverse frequency of the tower. However, in the spectra of the tower tops, the apparent frequency of transverse tower and vertical deck interaction always appears and it is the same frequency as that of vertical motions of the deck.
(4) From the earthquake records, it was not possible to identify the frequency of the tower (alone) in the longitudinal direction as was done by Abdel-Ghaffar et al. (1985). However, in the spectra, the apparent frequency of longitudinal tower interaction with vertical deck is identified and is the same frequency as that of deck.
(5) These are identified by the respective authors as first antisymmetric modes. The authors explain that the low-frequency content of ambient data, most likely containing the symmetrical mode could not be identified due to noise content.

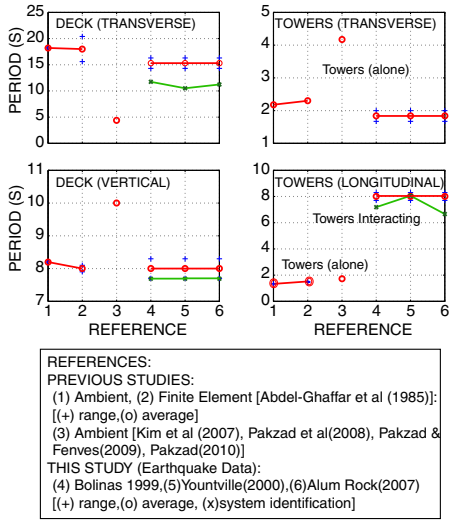

Figure 19. Summary of ambient data analyses (references 1 and 3), mathematical finite element modal analyses (2), and analyses of low-amplitude earthquake response data (4–6) showing ranges and averages (if applicable) for each reference data source. For the low-amplitude earthquake data analyses the shorter periods are more consistent for transverse and vertical motions of the deck. Note that, results from reference 3 are considerably different most likely due to low signal-to-noise ratio of ambient data for low frequencies (Pakzad and Fenves 2009).

studies performed using mathematical models and ambient data. For some of the important modes, there appears to be little consistency among the frequencies determined by the different methods; however, the frequencies determined from recorded earthquake responses are generally more consistent. Previous studies have demonstrated similar inconsistencies between the dynamic characteristics of buildings determined from strong shaking and from low-amplitude vibration data (Çelebi et al. 1993, Çelebi 2007). Furthermore, as Abdel-Ghaffar and Scanlan (1985a, b) have also inferred, the fundamental frequencies are present in the spectra of data from several key locations due to interaction of tower, cable, suspenders, and deck. Such interaction was also observed in data recorded at another long-span bridge (e.g., Bill Emerson Memorial Bridge at Cape Girardeau, MO; Çelebi 2006).

The results by Kim et al. (2007), Pakzad et al. (2008, 2009), and Pakzad (2010) are considerably different for some modes than those of Abdel-Gahffar et al. (1985) and this study. The main reason for the differences, as stated in Pakzad and Fenves (2009), is "large low-frequency content in transverse direction, which is not distinguishable from noise, so the first transverse mode, expected to be symmetric, cannot be identified." Although not stated in Pakzad and Fenves (2009), the figures for the vertical modes at 0.106 Hz also show that it belongs to antisymmetric vertical mode, possibly due to same reason.

In Figure 19, the fundamental periods of the deck transverse and vertical motions and the two towers' transverse and longitudinal motions are graphically presented to show that the values determined using earthquake data (from both spectral and system identification

analyses) are consistently lower than those for the ambient and mathematical modal analyses. This is the opposite of what is normally observed when comparing responses from ambient vibrations to those from seismic motions. No clear explanation for this discrepancy can be made at this time.

CONCLUSIONS

This is the first study of the Golden Gate Bridge in San Francisco, California, using small-amplitude response data from three earthquakes recorded by the GGB seismic array. The raw data obtained from the public domain data center (www.strongmotioncenter.org) has been reprocessed with a much lower corner frequency in order to extract the expected low-frequencies of a long-span suspension bridge such as the GGB.

Some of the principal modal frequencies (periods) are identified at key locations and along key directions of the bridge using spectral and system identification analyses. These results are compared to those of other previous studies which used data obtained from ambient tests as well as from mathematical models.

The bridge is undergoing retrofit, and thus analyses based on the available data will serve as a baseline for studies of any response data obtained following completion of the retrofit of the bridge.

Interaction of the tower top, cable, and deck during an earthquake are inferred from the similarity in frequencies along different directions of the bridge. This type of interaction has also been noted in past studies with ambient data (as well as on other cabled bridges).

It is concluded that center deck (vertical [~0.12–0.13 Hz] and transverse [~0.06–0.07 Hz]) frequencies are dominant low frequencies and are also the apparent frequencies due to the interaction between deck, cables, and towers. Towers exhibit their own frequencies, but also the deck frequencies because of interaction. Since the differences between the frequencies of the towers and deck are large, deck frequencies are the same as apparent interaction frequencies of the interacting tower, cable, and deck system of the suspension bridge. This is an important conclusion of the study. "Stand-alone" tower frequencies are ~0.2 Hz (longitudinal) and ~0.5–0.6 Hz (transverse).

In general, the earthquake data analyses result in higher apparent frequencies (shorter periods) than those determined by the prior studies of Abdel-Ghaffer et al. (1985) using ambient data and mathematical models. This is the reverse of what is normally expected. No clear explanation for this result can be given at this time. On the other hand, Pakzad and Fenves (2009) obtained a higher period for the vertical mode of the suspension span deck and lower period for the transverse mode of the deck—both modes belonging to antisymmetrical modes of the deck. They found the transverse mode of towers to have a higher period for the first mode.

Although the results are not entirely consistent, they may shed light on what variability of lower frequencies (longer periods) is to be expected from much stronger shaking with larger signal-to-noise ratios. Such motions may be generated from a larger earthquake at a closer distance and should no doubt excite some of the modes more strongly than the low-amplitude

motions. Variations in the level of shaking during ambient conditions and due to the low-amplitude earthquakes may also cause the identified variations of fundamental frequencies.

A few additional nonredundant sensors are necessary to better define the various symmetrical and antisymmetrical modes defined in Figure 3. At a minimum, symmetrical vertical channels next to Channels 15 and 29, a vertical pair at ¾ center span of the deck between mid-span and north tower, and additional transverse channels at these same locations can contribute to a better and more complete evaluation of some of the key dynamic characteristics at key components of the bridge, and to better assessing the interaction between the components. To illustrate the importance of these additions to the array of sensors, it is noted that, during the 1944–1946 period with the limited number of bulky accelerometers, emphasis in their deployments have been placed on the deck as follows: two each at ¼, ½, and ¾ point locations and one at 3/8 location from south to north of the main-span, and two at ½ point location of the south side-span of the bridge (Vincent 1958).

ACKNOWLEDGEMENTS

The author thanks internal USGS reviewers for their comments and suggestions that improved this paper. The author also thanks the California Strong Motion Instrumentation Program (CSMIP) of the California Geological Survey (CGS) for making additional raw data available from events via the new site www.strongmotioncenter.org. Special thanks are due to Chris Stephens, Manager of Strong Motion Data Center at USGS, for carefully reprocessing the low amplitude earthquake response data of GGB used in this study.

REFERENCES

Abdel-Ghaffar, A., and Scanlan, R., 1985a. Ambient vibration studies of Golden Gate Bridge: I. suspended structure, *Journal of Engineering Mechanics* **111**, 463–482.

Abdel-Ghaffar, A., and Scanlan, R., 1985b. Ambient vibration Studies of Golden Gate Bridge: II. pier-tower structure, *Journal of Engineering Mechanics* **111**, 483–499.

Abdel-Ghaffar, A., Scanlan, R., and Diehl, J., 1985. *Analyses of the Dynamic Characteristics of the Golden Gate Bridge by Ambient Vibration Measurements*, Princeton University Report: 85-SM-1, February 1985, 354 pp.

Baron, F., Arikan, M., and Hamati, E., 1976. *The Effects of Seismic Disturbances on the Golden Gate Bridge*, Report No. EERC 76-31, Earthquake Engineering Research Center, University of California, Berkeley.

Bendat, J. S., and Piersol, A. G., 1980. *Engineering Applications of Correlation and Spectral Analysis*, John Wiley and Sons, New York, 472 pp.

Çelebi, M., Phan, L., and Marshall, R., 1993. Dynamic characteristics of five tall buildings during strong and low-level amplitude motions, *International Journal of Design of Tall Buildings*, John Wiley and Sons, Ltd, March 1993.

Çelebi, M., 2006). Real-time seismic monitoring of the new Cape Girardeau (MO) Bridge and preliminary analyses of recorded data: An overview, *Earthquake Spectra* **22**, 609–630.

Çelebi, M., 2007. On the variation of fundamental frequency (period) of an undamaged building – a continuing discussion, *Int'l. Conf. on Experimental Vibration analyses for Civil Engineering Structures*.

Çelebi, M., 2010. Golden Gate Bridge response–a preliminary study with low-amplitude data from three earthquakes, paper accepted, *14th European Conference of Earthquake Engineering*, Ohris, Macedonia, August 28–Sept. 3, 2010.

Chopra, A., 1996. *Dynamics of Structures: Theory and Applications of Earthquake Engineering*, Prentice Hall, Upper Saddle River, NJ, 844 pp.

Jacobsen, L. S., and Ayre, R. S., 1958. *Engineering Vibrations*, McGraw-Hill, New York, 564 pp.

Kim, S., Pakzad, S., Culler, D., Demmel, J., Fenves, G., Glaser, S., and Turon, M., 2007. Health monitoring of civil infrastructures using wireless sensor networks, *Proceedings of the Int'l Conf. on Information Processing in Sensor Networks (IPSN '07)*, Cambridge, MA., ACM Press, 254–264.

Ljung, L., 1987. *System Identification: Theory and User*, Prentice Hall, Upper Saddle River, NJ, 672 pp.

Luco, J. E., Wong, H. L., and Trifunac, M. D., 1986. *Soil-Structure Interaction Effects on Forced Vibration Tests*, Department of Civil Engineering Report No 86-05, University of Southern California, Los Angeles.

The MathWorks, Inc., 1988. System Identification Toolbox for use with MATLAB, *MATLAB User's Guide*, The MathWorks, Inc., South Natick, MA.

Pakzad, S. N., Fenves, G. L., Kim, S., and Culler, D. E., 2008. Design and implementation of scalable wireless sensor network for structural monitoring, *ASCE Journal of Infrastructure Engineering* **14**, 89–101.

Pakzad, S. N., and Fenves, G. L., 2009. Statistical analysis of vibration modes of a suspension bridge using spatially dense wireless sensor network, *ASCE Journal of Structural Engineering* **135**, 863–872.

Pakzad, S. N., 2010. Development and deployment of large scale wireless sensor network on a long-span bridge, *Smart Structures and Systems* **6**, 525–543.

Trifunac, M. D., Ivanovic, S. S., and Todorovska, M. I., 2001. Apparent periods of a building: Fourier analyses, *AASCE Journal of Structural Division* **127**, 517–526.

Vincent, G. S., 1958. Golden Gate Bridge vibration studies, *Journal of Structural Division*, ASCE, **84**, Paper 1817.

Vincent, G. S., 1962a. Correlation of predicted and observed suspension bridge behavior, *Transactions*, ASCE, **127**, 646–666.

Vincent, G. S., 1962b. Golden Gate Bridge vibration studies, *Transactions*, ASCE, **127**, 667.

(Received 4 December 2010; accepted 23 June 2011)